Gauge Field and the Confinement-Deconfinement Transition in Hydrogen-Bonded Ferroelectrics

Chyh-Hong Chern[1,*] and Naoto Nagaosa[2,3]
[1]Department of Physics, National Taiwan University, Taipei 10617, Taiwan
[2]Department of Applied Physics, University of Tokyo, Tokyo 113-8656, Japan
[3]RIKEN Center for Emergent Matter Science (CEMS), Wako 351-0198, Japan
(Received 19 January 2013; published 17 June 2014)

Quantum melting of a ferroelectric moment in the frustrated hydrogen-bonded system with the "ice rule" is studied theoretically by using quantum Monte Carlo simulation. The large number of nearly degenerate configurations are described as the gauge degrees of freedom; i.e., the model is mapped to a lattice gauge theory, which shows the confinement-deconfinment transition (CDT). The dipole-dipole interaction J_2, on the other hand, explicitly breaks the gauge symmetry leading to the ferroelectric transition at finite temperature T. It is found that the crossover from the FT to CDT manifests itself in the reduced correlation length of the polarization $\xi_{\mathrm{FT}} \sim \Delta(K - K_c)^{-\nu}$, with $\Delta \propto \sqrt{J_2}$ while K_c and ν remains finite in the limit $J_2 \to 0$. In contrast, the Curie-Weiss-like law for the susceptibility χ and the spontaneous polarization behaves smoothly and the length scale ξ_{CDT}, related to the molecular symmetry and volume for CDT, does not reduce in this limit.

DOI: 10.1103/PhysRevLett.112.247602 PACS numbers: 77.80.B-, 11.15.-q, 64.60.F-

The hydrogen-bonded systems are ideal laboratories to study quantum tunneling. The ferroelectric properties of these systems have attracted a lot of attention since the old work of Slater on KH_2PO_4 (KDP) [1]. The quantum melting of the ferroelectric order to result in the quantum paraelectricity is a rather common phenomenon observed in several hydrogen-bonded ferroelectrics [2–5], which is usually described by the transverse Ising model

$$H = -\sum_{ij} J_{ij}\sigma_i^z\sigma_j^z - K\sum_i \sigma^x, \qquad (1)$$

where $\sigma^z = \pm 1$ specify the positions of the hydrogen atoms, J_{ij} is the dipole-dipole interaction, and K represents the tunneling matrix element. These two interactions compete with each other, and by increasing K, a phase transition from the ordered state to the quantum disordered phase occurs.

On the other hand, it often happens that the constraints are significant to the hydrogen-bonded systems. Actually, the hydrogen positions in the representative system KDP are already subject to the constraint, i.e., the so-called "ice rule" [1]. Namely, only two of the four hydrogen atoms next to a tetrahedron are approaching the center for the low-energy sector. A similar constraint is also relevant to the recently studied quasi-two-dimensional antiferroelectric squaric acid (H_2SQ), where the square molecule is surrounded by four molecules with hydrogen bonds [5], and the two-in-two-out configurations are energetically stable. This ice rule is the generalization of the hydrogen bonds in ice leading to the macroscopic degeneracy of the ground-state configurations as discussed by Pauling in the 1930s [6]. Therefore, an important issue is how this macroscopic degeneracy of the low-energy states in the hydrogen bonded systems affects the nature of the phase transition.

The constraints imposed on the physical variables are common phenomena found in many other cases. Frustrated magnets are one of such examples, where some of the macroscopically degenerate spin configurations are selected as the lowest energy states. Spin ice in a pyrochlore ferromagnet is a representative example, in which the hydrogen position is replaced by the direction of the spin, and the ice rule applies simultaneously in every tetrahedron. This property leads to an interesting phenomena, e.g., the absence of the long-range ordering down to zero temperature and the deconfined magnetic monopoles as the excitations [7]. These are described well by the gauge theory representing the constraints within the framework of the classical statistical mechanics. Quantum effects on the spin ice model have attracted a lot of interest recently [8,9].

In this Letter, we develop a theory for the organic ferroelectrics with macroscopic degeneracy. A Z_2 gauge-invariant term accounting for the ice rule is introduced explicitly [10]. Different from a $U(1)$ gauge theory, our model exhibits two types of quantum phase transitions, i.e., the confinement-deconfinement transition (CDT) of the gauge field and the ferroelectric transition (FT) of the local dipole moments. We relate these two phenomena by introducing a dipole-dipole interaction J_2 explicitly breaking the gauge symmetry [see Eq. (3)]. Because of the macroscopic degeneracy, different from the ordinary FT, we found two length scales ξ_{FT} and ξ_{CDT} (defined later) in the vicinity of the FT as the system is close to the CDT.

Taking the squaric acid as a prototype, we consider a two-dimensional model, $H = H_0 + H_1 + H_2$, where

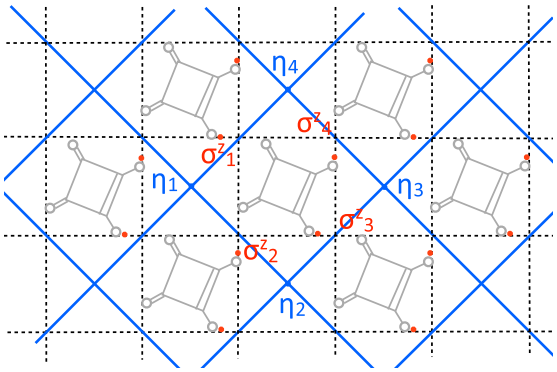

FIG. 1 (color online). The two-dimensional square lattice (blue lines) formed by the squaric acid molecules. The red circles label the hydrogen ions. The η variables are defined on the lattice sites. The hydrogen positions are parametrized by the σ^z variables, which are defined on the lattice bonds forming a two-dimensional dual lattice (black dashed lines).

$$H_0 = -J_0 \sum_{\square} \sigma_1^z \sigma_2^z \sigma_3^z \sigma_4^z - K \sum_i \sigma_i^x, \tag{2}$$

$$H_1 = J_1 \sum_{\square} (\sigma_1^z \sigma_3^z + \sigma_2^z \sigma_4^z), \qquad H_2 = -J_2 \sum_{\langle AB \rangle} \vec{P}_A \cdot \vec{P}_B \tag{3}$$

in the lattice in Fig. 1, where the summation of $\square$ in Eqs. (2) and (3) is over the plaquettes of the blue lattice in Fig. 1 resembling the H_2SQ molecules and the σ variables are defined on the bonds of the plaquettes [5]. On each lattice bond there is a hydrogen ion shared by two neighboring molecules representing the hydrogen bond. We use σ^z to parametrize the position of hydrogen ions in the following way: If a hydrogen is closer to molecule A, it is the "+" state, otherwise it is a "−" state, representing a gauge field. The H_2 in Eq. (3) represents the nearest-neighbor dipole-dipole interaction, and the components of the dipole moment $\vec{P}_i$ are defined by $P_{(A,B)x} = (\pm)\frac{1}{4}(\sigma_1^z + \sigma_2^z - \sigma_3^z - \sigma_4^z)$ and $P_{(A,B)y} = (\pm)\frac{1}{4}(\sigma_2^z + \sigma_3^z - \sigma_1^z - \sigma_4^z)$, where $(+)$ is for molecule A and $(-)$ is for molecule B.

The ice rule constrained by the gauge term J_0 and the Ising term J_1 generates a macroscopic degeneracy, which is distinct from the one in the antiferromagnetic Ising model in the 2D pyrochlore (checkerboard) lattice [11] and the quantum vertex model [12,13]. The gauge term favors eight different configurations in the low-energy sector illustrated in Fig. 2. Note that this quantum Hamiltonian H_0 corresponds to the $(2+1)$-dimensional Ising gauge theory in the temporal gauge; i.e., the time component of the gauge field is fixed to be one. The addition of the J_1 term lifts the degeneracy so that the states of Figs. 2(e)–2(h) remain. They are particularly interesting because they carry finite dipole moments. For example, the direction of the dipole moments for molecule A are shown by red arrows in Fig. 2.

The finite-temperature property due to the gauge term was studied previously by Maier *et al.* [10]. Here, we focus

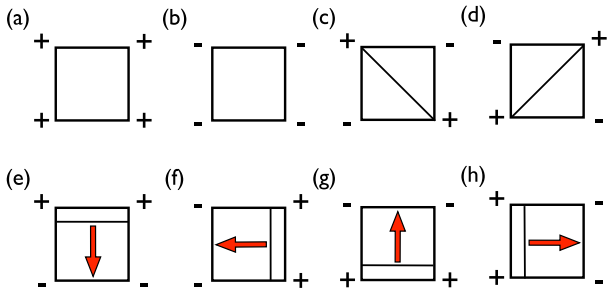

FIG. 2 (color online). The ground-state configuration of each plaquette in the model of H_0 in Eq. (2). There are finite dipole moments in the states (e)–(h), but not in the states (a)–(d). The directions of the dipole moment are drawn in red for the molecules of group A.

on the quantum phase transition in the presence of the transverse field. The quantum phase diagram at zero temperature can be summarized in Fig. 3. When $J_1 = J_2 = 0$, there is a second-order CDT at critical K_c [14,15]. At first glance, the introduction of the J_1 term breaks the gauge symmetry and the CDT. However, there remains a hidden gauge symmetry. To see this, one can introduce the η variables defined in the dual lattice in Fig. 1. Redefining the σ^z variable as $\sigma_j^z = \eta_i \eta_j$ in a restricted Hilbert space of the minimum J_0 energy, for $J_2 = 0$, we obtain the action

$$S = -\beta J_0 + \frac{2\beta J_1}{n} \sum_{\square} \eta_i \eta_j \eta_k \eta_l - K' \sum_{\square'} \eta_i \eta_j \eta_{i'} \eta_{j'}, \tag{4}$$

where $\square$ ($\square'$) are the plaquettes in the spatial (imaginary-time) direction in the dual lattice, n is the dimension in the imaginary-time direction, and $\beta = 1/(k_B T)$. In Eq. (4), we express the σ^x term in the η variables with $K' = \log[\coth(\beta K/n)]/2$. The hidden symmetry protects the CDT to extend to the finite J_1 region. We also perform

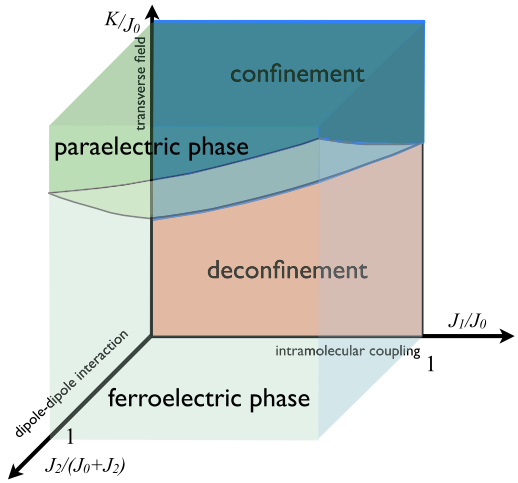

FIG. 3 (color online). The zero-temperature phase diagram. For $J_2 = 0$, there are two phases separated by a confinement-deconfinement phase transition. For finite J_2, the phase space is divided by a second-order ferroelectric phase transition.

the quantum Monte Carlo calculation to confirm this. The numerical results are prepared in the Supplemental Material [16]. Our analysis indicates that the CDT is a robust transition, distributed over a wide range in the phase diagram where the ice rule is satisfied. As a first result, the phase diagram is divided into the deconfined phase and the confined phase in the $J_2 = 0$ plane.

Even without the dipolar interaction J_2, the dielectric susceptibility in the novel deconfined phase diverges for $K \leq K_c$ at $T = 0$. In Fig. 4, we perform the Monte Carlo calculation to compute the correlation in the imaginary-time direction, defined by

$$C_\tau = \frac{1}{N}\sum_i \langle P_x(i,\tau)P_x(i,0)\rangle, \tag{5}$$

where τ is the coordinate in the imaginary-time direction. The temperature $k_B T = 0.02 J_0$ and the range of τ is $10 < \tau < 30$ in Fig. 4. The Monte Carlo simulation is performed in the lattice up to 32×32 sites in 10^6 Monte Carlo steps. The details of the Monte Carlo simulations are given in the Supplemental Material [16]. Under the temporal gauge, Eq. (5) contains gauge-invariant terms; i.e., $\langle \sigma_i(\tau)\sigma_i(0)\rangle \neq 0$. Thus, C_τ does not vanish due to the gauge symmetry at $J_2 = 0$. We obtain that C_τ has a power-law decay for $K < K_c$ and C_τ has an exponential decay for $K > K_c$. Therefore, the dielectric susceptibility,

$$\chi = \frac{1}{N}\sum_{i,j}\int_0^\beta d\tau \langle P_x(i,\tau)P_x(j,0)\rangle, \tag{6}$$

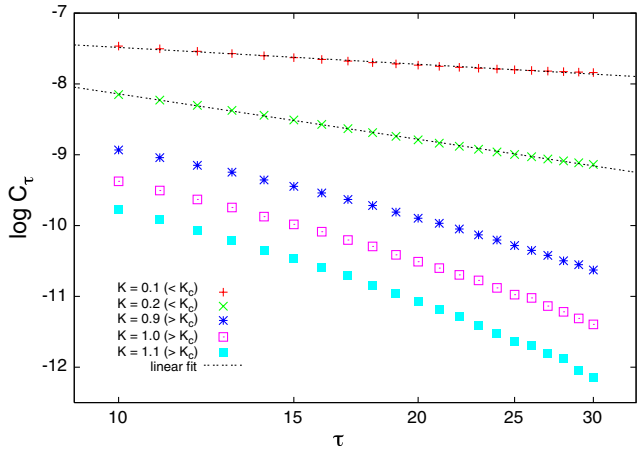

FIG. 4 (color online). The logarithmic plot of the correlation in the imaginary-time direction at $J_2 = 0$, where CDT takes place. τ is the coordinate in the imaginary-time direction. Using $J_1 = 0.2J$, the K_c of CDT at $J_2 = 0$ is 0.64, as shown in the inset of Fig. 5. We plot the results for $K = 0.1$ and 0.2 ($< K_c$) to demonstrate the power-law behavior in the deconfined phase and $K = 0.9$, 1.0, and 1.1 ($> K_c$) to show the exponential decay in the confined phase. Note that C_τ is independent of τ for $K = 0$, and the numerical error is 0.1%–1%.

diverges for $K \leq K_c$ at $T = 0$. We note that at $K = 0$ the system is classical and $\chi \sim 1/T$, also diverging at $T = 0$.

Introducing the dipolar interaction $J_2 \neq 0$, the ground state develops a spontaneous polarization for $K < K_c(J_2)$. At finite temperature, a ferroelectric transition can occur. Correspondingly, χ diverges at the critical temperature T_c and the power-law behavior of χ as $T \to 0$ disappears. Moreover, a quantum phase transition to the dielectric state can be driven by increasing K. In Fig. 5, χ is computed for six different J_2 values. The dielectric susceptibility satisfies the Curie-Weiss-like behavior $\chi = C(K - K_c)^{-1}$ for *all* J_2, and K_c vary with J_2 as shown in the inset, which establishes our first relation between CDT and FT. The confined phase at $J_2 = 0$ and the dielectric phase for finite J_2 share a similar K dependence. C, shown in the inset of Fig. 5, are *independent of* J_2, and K_c of FT converges to a finite value, indicating that the FT is robust and the dipolar interaction J_2 is a relevant perturbation. The convergent value of K_c at $J_2 = 0$ is the one for CDT taking place. Extending to the finite J_2 region, the deconfined phase at the zero-J_2 plane becomes the ferroelectric phase, and the confined phase becomes the dielectric phase as depicted in Fig. 3. Because of these nontrivial connections, how the criticality of the confinement-deconfinement phase transition of the gauge field affects the criticality of the ferroelectric phase transition is the main scope of this Letter.

To answer this, we compute the ferroelectric correlation length ξ_{FT}, defined by

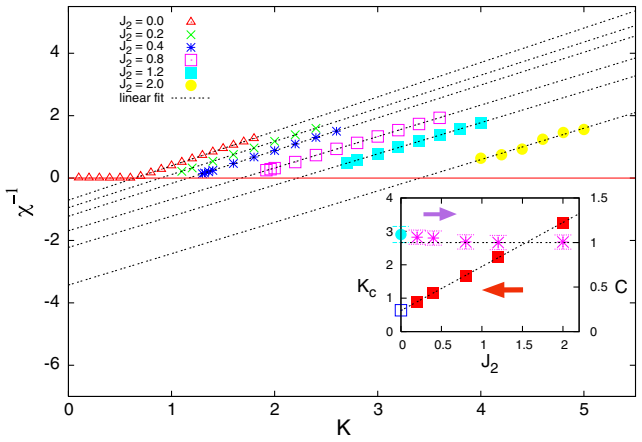

FIG. 5 (color online). The inverse of the dielectric susceptibility χ^{-1} for various J_2 values is computed for $J_0 = 1$ and $J_1 = 0.2$ at $T = 0.05J_0$. The dielectric susceptibility satisfies well the Curie-Weiss-like behavior $\chi = C/(K - K_c)$ for $K > K_c$. We plot, in particular, the full range of K for the $J_2 = 0$ case to show the divergence of the susceptibility for $K < K_c$. In the inset, we extract C and K_c as functions of J_2. The data of C use the right-hand y axis and K_c uses the left-hand axis. C remains unity for all J_2. K_c has a linear relation with J_2, terminating at $K_c = 0.64$ for $J_2 = 0$, where the confinement-deconfinement phase transition takes place. Note that the numerical error is ~0.2%.

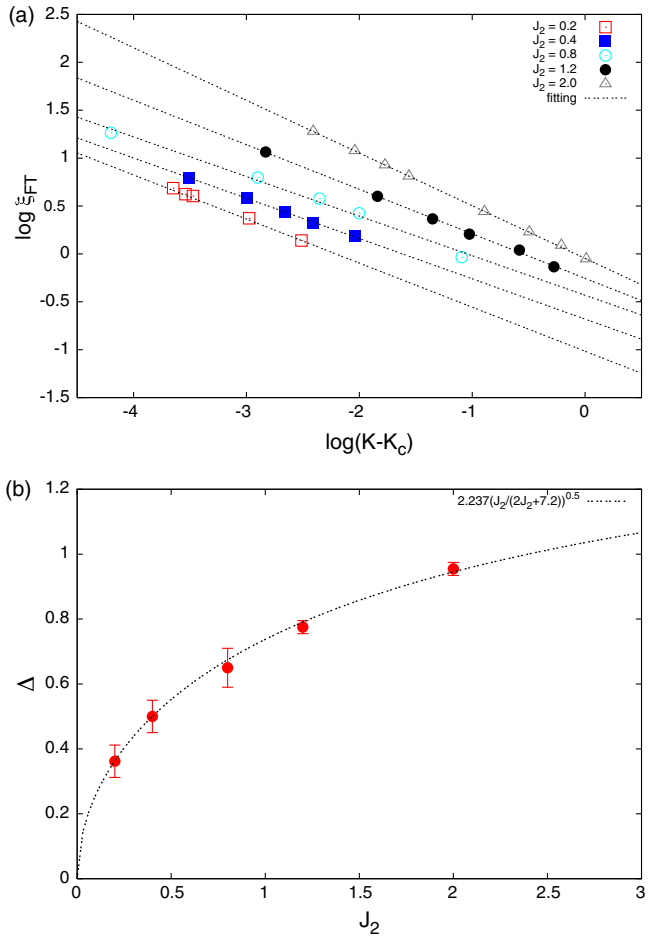

FIG. 6 (color online). (a) The logarithmic plot of the correlation length ξ_{FT}. ν is obtained as 0.55, 0.46, 0.41, 0.42, 0.46 for $J_2 = 2.0, 1.2, 0.8, 0.4, 0.2$, respectively. (b) The coefficient Δ as a function of J_2. The dotted curve is the fitting by the mean-field result.

$$\langle P_s(r)P_s(0)\rangle \propto \frac{e^{-r/\xi_{\mathrm{FT}}}}{r}, \qquad s = x \quad \text{or} \quad y, \qquad (7)$$

for $K > K_c$ in Fig. 6. The FT is a second-order phase transition because both the dielectric constant and the correlation length diverge at $K = K_c$. As shown in Fig. 6(a), ξ_{FT} obeys $\sim\Delta/(K - K_c)^{\nu}$ very nicely, with $\nu = 0.46, 0.42, 0.41, 0.46, 0.55$ for $J_2 = 0.2, 0.4, 0.8, 1.2, 2.0$. We believe that the fluctuation of ν comes from error bars in the estimation. Those values of ν are closer to the mean-field values from the 3D Ising value $\nu \approx 0.6$, indicating that the systems are outside the critical region. For a conventional ferroelectric system without macroscopic ground-state degeneracy, Δ is a constant independent of the coupling constant J_2. However, we obtain $\Delta \sim \sqrt{J_2}$ as $J_2 \to 0$ in the numerical calculations and in the mean-field theory (detailed in the Supplemental Material [16]) as shown in Fig. 6(b). The connection between the FT and the CDT is highly nontrivial and can be understood as the following. As is well known, any physical quantity without gauge invariance has a zero ground-state expectation value in the gauge-invariant theory [14,15]. The correlation function at finite distance in Eq. (7) should be zero at $J_2 = 0$, since the $\langle \sigma_i^z \sigma_j^z \rangle$ for $i \neq j$ therein is not gauge invariant with respect to the spatial gauge transformation. Consequently, although the polarization moment C remains unity at $J_2 = 0$, not only does the system not order, but additiionally the spatial correlation is restricted to zero. In other words. the dipolar interaction in Eq. (3) introduces just the k dependence of the ferroelectric wave. When $J_2 = 0$, the system is free of spatial coupling and, therefore, ξ_{FT} vanishes. This profound feature provides a good measure of distance for a ferroelectric system in the vicinity of the CDT. The measurement of the spatial correlation length by neutron scattering or Raman scattering [17,18] toward the phase transition can be used to detect whether or not the system is near the CDT.

Bordered by the deconfined phase, the ferroelectric phase for small but finite J_2 is different from the conventional ferroelectric materials. The frustration due to the ice rule is constrained by the molecular symmetry and volume, which also extends to finite J_2. At $J_2 = 0$, it can be parametrized by the product of four σ^z's in a molecule, i.e., $p_i = \sigma_1^z \sigma_2^z \sigma_3^z \sigma_4^z$. In the critical region, the correlation $\langle p_i p_j \rangle$ is proportional to $R^{-(d-\alpha/\nu)} g(R/\xi_{\mathrm{CDT}})$, where $R = |R_i - R_j|$ is the distance between molecules i and j, while α and ν are the critical exponent for the specific heat and the correlation length of the corresponding 3D Ising model, respectively. The function g is a scaling function and ξ_{CDT} is the correlation length in the 3D Ising model, which diverges at $K = K_c$ [15]. The correlation naturally extends to the finite J_2 region. Therefore, there are two length scales behaving differently in the ferroelectric phase in the small J_2 region. As ξ_{FT} converges to the atomic scale, ξ_{CDT} remains finite at $J_2 = 0$. Representing the molecular symmetry, ξ_{CDT} can actually be measured in the nonresonance Raman scattering as discussed in the Supplemental Material [16].

In conclusion, the effect of the ice rule and consequent gauge symmetry in the hydrogen-bonded ferroelectrics is intricate. Although the confinement-deconfinement transition at $J_2 = 0$ cannot be described by the local order parameter, it can be indirectly probed by the measurement of the dielectric susceptibility. For $K > K_c$, the system is in the confined phase with the dielectric susceptibility obeying a Curie-Weiss-like law. For $K \leq K_c$, the system is in the deconfined phase with a divergent dielectric susceptibility. As soon as the dipolar interaction J_2 is turned on, the ferroelectric phase develops for $K \leq K_c$ as T is lowered. When the dipolar interaction is small, the approximate gauge invariance suppresses the growth of the critical region by regulating the spatial correlation length ξ_{FT} obeying $\sim\Delta(K - K_c)^{-\nu}$. We demonstrate $\Delta \sim \sqrt{J_2}$ both in the numerical simulation and in the mean-field treatment. Our theory provides a scheme to uncover the shadow of the gauge field as well as to realize the accompanying CDT by

identifying the two length scales ξ_{FT} and ξ_{CDT} near the ferroelectric phase transition. A future research direction can be a further extension to include the long-ranged dipolar interaction. Most importantly, a theory to describe the class of FT belonging to the first-order phase transition should be developed.

The authors acknowledge fruitful discussion with Y. Tokura. This work is supported by a Grant-in-Aid for Scientific Research (Grant No. 24224009) from the Ministry of Education, Culture, Sports, Science and Technology of Japan, the Strategic International Cooperative Program (Joint Research Type) from Japan Science and Technology Agency, and the Funding Program for World-Leading Innovative RD on Science and Technology (FIRST Program) (N. N.). It is also supported by the National Science Council of Taiwan under Grant No. NSC 100-2112-M-002-015-MY3 (C.-H. C.). C.-H. C. is grateful for the travel support from the Center for Theoretical Sciences in NTU.

*Corresponding author.
chchern@ntu.edu.tw

[1] J. C. Slater, J. Chem. Phys. **9**, 16 (1941).
[2] G. A. Samara, Ferroelectrics **71**, 161 (1987).
[3] G. A. Samara, Phys. Rev. Lett. **27**, 103 (1971).
[4] P. S. Peercy and G. A. Samara, Phys. Rev. B **8**, 2033 (1973).
[5] Y. Moritomo, Y. Tokura, H. Takahashi, and N. Mori, Phys. Rev. Lett. **67**, 2041 (1991).
[6] L. Pauling, J. Am. Chem. Soc. **57**, 2680 (1935).
[7] C. Castelnovo, R. Moessner, and S. L. Sondhi, Nature (London) **451**, 42 (2008).
[8] K. A. Ross, L. Savary, B. D. Gaulin and L. Balents, Phys. Rev. X **1**, 021002 (2011).
[9] N. Shannon, O. Sikora, F. Pollmann, K. Penc, and P. Fulde, Phys. Rev. Lett. **108**, 067204 (2012).
[10] H.-D. Maier, H. E. Müser, and J. Petersson, Z. Phys. B **46**, 251 (1982).
[11] N. Shannon, G. Misguich, and K. Penc, Phys. Rev. B **69**, 220403(R) (2004).
[12] O. F. Syljuåsen and S. Chakravarty, Phys. Rev. Lett. **96**, 147004 (2006).
[13] E. Ardonne, P. Fendley, and E. Fradkin, Ann. Phys. (Amsterdam) **310**, 493 (2004).
[14] J. B. Kogut, Rev. Mod. Phys. **51**, 659 (1979).
[15] R. Savit, Rev. Mod. Phys. **52**, 453 (1980).
[16] See Supplemental Material at http://link.aps.org/supplemental/10.1103/PhysRevLett.112.247602, which includes Ref. [19], for the detail results from the Monte Carlo calculations.
[17] Y. Okimoto, R. Kumai, S. Horiuchi, H. Okamoto, and Y. Tokura, J. Phys. Soc. Jpn. **74**, 2165 (2005).
[18] G. F. Reiter, J. Mayers, and P. Platzman, Phys. Rev. Lett. **89**, 135505 (2002).
[19] H. W. J. Blote and Y. Deng, Phys. Rev. E **66**, 066110 (2002).